Multiobjective Optimization of an Industrial Wiped-Film Pet Reactor

V. Bhaskar, Santosh K. Gupta, and Ajay K. Ray
Dept. of Chemical and Environmental Engineering, National University of Singapore, 10 Kent Ridge Crescent, Singapore—119260, Singapore

Multiobjective optimization of a third-stage, wiped-film polyester reactor was carried out using a model that describes an industrial poly(ethylene terephthalate) reactor quite well. The two objective functions minimized are the the acid and vinyl end group concentrations in the product. These are two of the undesirable side products produced in the reactor. The optimization problem incorporates an endpoint constraint to produce a polymer with a desired value of the degree of polymerization. In addition, the concentration of the di-ethylene glycol end group in the product is constrained to lie within a certain range of values. Adaptations of the nondominated sorting genetic algorithm have been developed to obtain optimal values of the five decision variables: reactor pressure, temperature, catalyst concentration, residence time of the polymer inside the reactor, and the speed of the agitator. The optimal solution was a unique point (no Pareto set obtained). Problems of multiplicity and premature convergence were encountered. A ''smoothening'' procedure is suggested to generate near-optimal operating conditions. The optimal solution corresponds simultaneously to minimum values of the residence time of the polymeric reaction mass in the reactor.

Introduction

Process industries aim at maximizing their production capacities while simultaneously maintaining the product quality. Usually, there exists a trade-off between these two requirements. This is particularly true in the manufacture of polymers where the properties of the product are crucial and reactors have to be operated under conditions that yield products that satisfy relatively narrow specifications. At the same time, the operating variables must be at optimal condition to maximize the throughput. It is well established that the average molecular weight of the polymer produced determines several of the material's important physical properties, for example, strength and impact resistance. In addition, the concentrations of a few side products need to be below low limits or between narrow limits to ensure some other properties, like color and dyeability, to lie within specifications. Thus, the design and operation of polymerization reactors require optimization using multiple-objective functions and constraints, which are often conflicting.

Several studies have been reported in the literature on the optimization of polymerization reactors. These have been reviewed by Farber (1989) and Tieu et al. (1994). Most of these studies involve single (scalar) objective functions, incorporating several objectives with weightage factors. This parametric approach is quite inefficient and also has the drawback of possibly losing certain optimal solutions when the nonconvexity of the objective function gives rise to a duality gap (Goicoechea et al., 1982; Chankong and Haimes, 1983), something that is very difficult to verify for complex, real-life problems. The use of multiobjective optimization with objective functions that are vectors is a much better approach.

A few studies have been reported on the multiobjective optimization of polymerization reactors: Tsoukas et al. (1982), Farber (1986, 1989), Fan et al. (1984), Butala et al. (1988) and Choi and Butala (1991) have performed multiobjective optimization of copolymerization reactors. These early stud-

Correspondence concerning this article should be addressed to A. K. Ray.
Current address of S. K. Gupta: Dept. of Chemical Engineering, University of Wisconsin, Madison, WI 53706, on leave from the Indian Institute of Technology, Kanpur, 208016, India.

ies used the Pontryagin minimum principle or a pattern-search technique coupled with the ϵ-constraint method (Chankong and Haimes, 1983) to obtain Pareto optimal sets of nondominant solutions (a Pareto set is defined as follows: when we go from any one point to another, at least one objective function improves and at least one other worsens, Chankong and Haimes, 1983). Wajge and Gupta (1994) obtained optimal temperature histories corresponding to different points on the Pareto optimal sets for a nonvaporizing nylon-6 batch reactor, using similar techniques. Sareen and Gupta (1995) obtained optimal pressure histories and optimal values of the jacket fluid temperature at different points on the Pareto set for an industrial nylon-6 semibatch reactor where vaporization of monomer and water occurs, and is controlled by the pressure history, one of the decision variables. More recently, our group (Chakravarthy et al., 1997; Mitra et al., 1998; Garg and Gupta, 1999; Garg et al., 1999; Gupta and Gupta, 1999) have carried out multiobjective optimization studies on nylon-6 and polymethyl methacrylate (PMMA) reactors using a different, more robust technique, namely, an adapted version of the genetic algorithm (GA). This is the nondominated sorting genetic algorithm (NSGA), as developed by Srinivas and Deb (1995), and its modifications (Mitra et al., 1998), which enable it to be applied to problems where the decision variables are continuous *functions* rather than single discrete *values*. Pareto sets of nondominated solutions have been generated in all cases. The Pareto sets usually obtained in multiobjective optimization help channelize the thinking of a decision maker since they narrow down the choices from among which the ''preferred'' solution can be chosen using intuition, the latter often being nonquantifiable (Chankong and Haimes, 1983).

It is interesting to note that all these studies on multiobjective optimization have been on polymerization systems, and have appeared in specialty journals. Very little work in this area has been reported in the mainstream chemical engineering literature even though interesting and challenging problems exist, several of significant industrial importance. In this article, work on the multiobjective optimization of an important industrial operation, namely, polyester manufacture, is presented, and it is hoped that this will spur similar activity on other systems in chemical engineering. It can be emphasized that multiobjective optimization of real-life systems is quite complex and each new application may require the development of several adaptations of optimization algorithms to obtain meaningful solutions, irrespective of which mathematical procedure is used for the purpose. Indeed, a few such adaptations of the GA have been developed in earlier studies, and these have been found to be quite robust for solving multiobjective optimization problems (Goldberg, 1989; Deb, 1995). In this work some new adaptations also have been developed and presented that can be used for solving other similar problems.

In the present study, we consider the optimization of reactors producing fiber-grade polyethylene terephthalate (PET). As the petroleum/petrochemical/polymer sector is going through a lean period, any form of cost-cutting measure, which can be basically achieved from process optimization, would be beneficial for the polyester fiber industry. Commercially, PET is manufactured in three stages, using continuous reactors. The first (esterification) stage is carried out at atmospheric pressure and at 270–280°C. The raw materials commonly used are a molar excess of ethylene glycol (EG) and either purified terephthalic acid (PTA) or dimethyl terephthalate (DMT). Our study is based on the now popular PTA route. PTA and EG are usually processed in a series of CSTRs or a plug-flow reactor with a recycle in the first stage. A polycondensation catalyst, antimony trioxide, is injected in small concentrations (0.03–0.05% by weight) into the oligomer stream leaving this reactor. The second (prepolymerization) stage is carried out either in one or two agitated vessels under reduced pressures, at about 2–4 kPa (15–30 mm Hg) and 270–280°C. The degree of polymerization (DP) attains a value of about 30–40 in this stage. The prepolymer so produced undergoes final polycondensation in a finishing (or third-stage, wiped-film) reactor in which the pressure is maintained quite low at 0.133–0.266 kPa (1–2 mm Hg), at temperatures of about 285–295°C. Since the reaction mass is very viscous under these conditions, the finishing reactor has a special construction to enhance mass transfer and the removal of byproduct, ethylene glycol, in order to drive the reaction in the forward direction and to yield a product having a high value of DP. The finisher is usually a jacketed cylindrical vessel with a horizontal agitator, with large screens mounted on the latter. The reaction mass in the third-stage reactor is usually heated by condensing vapors in a jacket.

Several studies on the modeling and simulation of the different stages of PET manufacture have been reported, as reviewed by Ravindranath and Mashelkar (1986). Very few studies (Kumar et al., 1984 a,b,c; Immanuel and Gupta, 1999), however, have appeared in the literature, on the optimization of any industrial reactor producing PET. Indeed, we believe that this is the first comprehensive study on the multiobjective optimization of the complex, wiped-film industrial reactor, which is probably the most important of the three stages, since it controls the final properties of the product. Also, the model for the reactor that we have used for optimization is far superior to earlier models in terms of describing the *industrial* operation. In our earlier study (Bhaskar et al., 2000), we modified the model proposed by Laubriet et al. (1991) to match the operation of an *industrial* wiped-film reactor and have *tuned* the model parameters using three sets of industrial data available to us. The tuned model (without any change in the model parameters) predicts the fourth set of data extremely well. Thus, it can be inferred that the model represents all the important physicochemical phenomena taking place in the reactor reasonably well, and can be used to optimize its operation.

Table 1 presents the reaction scheme commonly used (Ravindranath and Mashelkar, 1984; Laubriet et al., 1991), as well as the rate and equilibrium constants [some tuned, the others from the literature (Ravindranath and Mashelkar, 1984)] to explain the industrial data on the wiped-film reactor. The complete set of model equations (Bhaskar et al., 1999) is summarized in Table 2. Table 3 gives the feed conditions used for optimization of the operation of the industrial reactor. A sensitivity analysis was also carried out on the model (Bhaskar et al., 2000) to develop an intuitive understanding of the behavior of the industrial wiped-film reactor. This helped in developing a meaningful optimization problem involving several different sets of objective functions and end-point constraints associated with the requirement of

Table 1. Kinetic Scheme and Kinetic Parameters

Kinetic Scheme

1. Ester interchange reaction (main polycondensation)

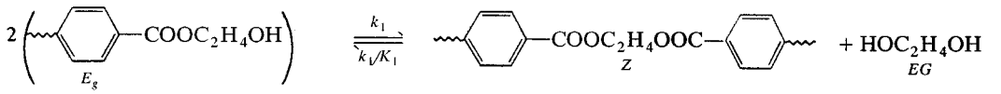

(1)

2. Acetaldehyde formation

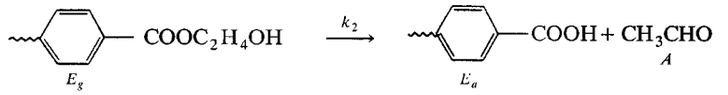

(2)

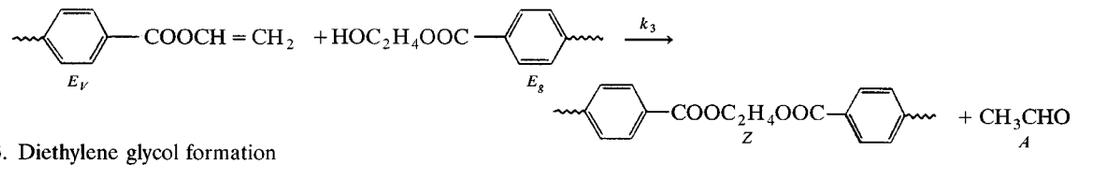

(3)

3. Diethylene glycol formation

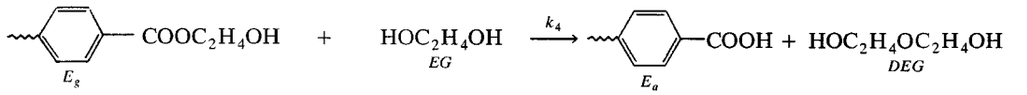

(4)

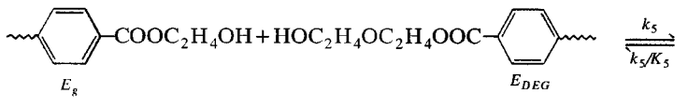

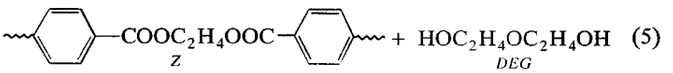

(5)

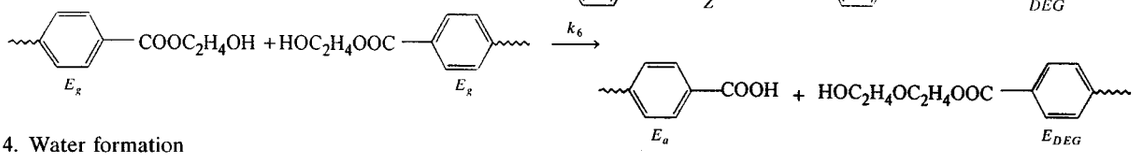

(6)

4. Water formation

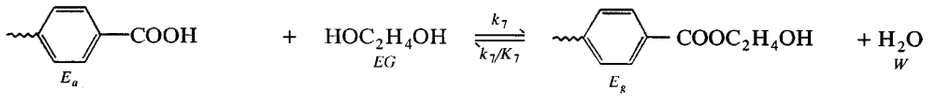

(7)

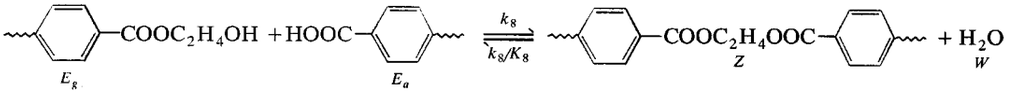

(8)

5. Degradation of Diester group

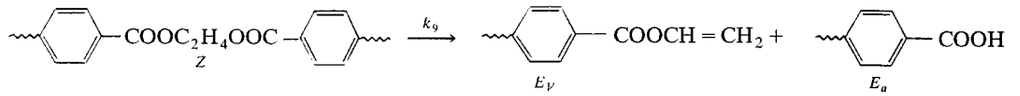

(9)

*Kinetic parameters** ($[Sb_2O_3] = 0.04$ wt. %)**

Reaction No.	Type of Reaction	Rate Constant $m^3/(mol\text{-}min)$	Equilibrium Constant
1	Reversible	$1.09\times10^3 \exp(-4{,}418/RT)$	6.1835
2	Irreversible	$4.7674\times10^7 \exp(-7{,}117/RT)^\dagger$	
3	Irreversible	$1.09\times10^3 \exp(-4{,}418/RT)$	
4	Irreversible	$8.32\times10^4 \exp(-7{,}117/RT)$	
5	Reversible	$1.09\times10^3 \exp(-4{,}418/RT)$	0.05143
6	Irreversible	$8.32\times10^4 \exp(-7{,}117/RT)$	
7	Reversible	$2.08\times10^3 \exp(-4{,}203/RT)$	2.5
8	Reversible	$2.08\times10^3 \exp(-4{,}203/RT)$	11.87
9	Irreversible	$0.2215\times10^9 \exp(-9{,}028/RT)^\dagger$	

*Laubiet et al. (1991).

**Values of k_{20}, k_{90}, K_1, K_5, and K_8 are those obtained in our previous study (Bhaskar et al., 1999), and differ from those of Lauriet et al. (1991).

$^\dagger min^{-1}$.

Table 2. Complete Set of Model Equations Used in this Study

Balance equations for the liquid phase

$$\frac{1}{\theta}\frac{d[E_g]}{dz} = [-2R_1 - R_2 - R_3 - R_4 - R_5 - 2R_6 + R_7 - R_8]$$

$$\frac{1}{\theta}\frac{d[E_a]}{dz} = [R_2 + R_4 + R_6 - R_7 - R_8 + R_9]$$

$$\frac{1}{\theta}\frac{d[Z]}{dz} = [R_1 + R_3 + R_5 + R_8 - R_9]$$

$$\frac{1}{\theta}\frac{d[E_v]}{dz} = [-R_3 + R_9]$$

$$\frac{1}{\theta}\frac{d[E_{DEG}]}{dz} = [-R_5 + R_6]$$

$$\frac{1}{\theta}\frac{d[EG]}{dz} = R_1 - R_4 - R_7 - k_l a([EG] - [EG^*])$$

$$\frac{1}{\theta}\frac{d[W]}{dz} = R_7 + R_8 - k_l a([W] - [W^*])$$

$$\frac{1}{\theta}\frac{d[DEG]}{dz} = R_4 + R_5 - k_l a([DEG] - [DEG^*])$$

where

$$R_1 = k_1[E_g]^2 - 4k_1'[Z][EG]$$
$$R_2 = k_2[E_G]$$
$$R_3 = k_3[E_v][E_g]$$
$$R_4 = 2k_4[E_g][EG]$$
$$R_5 = k_5[E_g][E_{DEG}] - 4k_5'[Z][DEG]$$
$$R_6 = k_6[E_g]^2$$
$$R_7 = 2k_7[E_a][EG] - k_7'[E_g][W]$$
$$R_8 = k_8[E_g][E_a] - 2k_8'[Z][W]$$
$$R_9 = k_9[Z]$$

Vapor–liquid equilibrium correlations

$$C_j^* = \left(\frac{C_{\text{poly}}}{1 - \sum_j x_j^*}\right) x_j^*; \qquad C_j^* = [EG^*], [W^*], [DEG^*]$$

$$C_{\text{poly}} = \frac{[E_g] + [E_a] + [E_v] + [E_{DEG}]}{2}$$

$$x_j^* = \frac{Py_j}{P_j^o \gamma_j}; \qquad j = EG, W, DEG$$

$$\ln P_{EG}^o = 49.703 - (8{,}576.7/T) - 4.042 \ln T$$

$$\ln P_W^o = 18.568 - \frac{4{,}047.606}{T - 33.3}$$

$$\ln P_{DEG}^o = 17.0326 - \frac{4{,}122.52}{T - 122.5}$$

$$y_j = \frac{\int_0^1 k_l a(C_j - C_j^*)\, dz}{\sum_j \int_0^1 k_1 a(C_j - C_j^*)\, dz + \int_0^1 (k_2[E_g] + k_3[E_v][E_g])\, dz} \quad j = EG, W, DEG$$

$$\gamma_j = \frac{1}{m_j}\exp\left(1 - \frac{1}{m_j} + \chi_1\right); \qquad j = EG, W, DEG$$

$$m_j = \frac{V_p \rho_j}{M_j}; \qquad j = EG, W, DEG$$

$$U_v = \sum_j \frac{M_j C_j}{\rho_j}; \qquad j = EG, W, DEG$$

$$V_p = \frac{1 - U_v}{C_{\text{poly}}}$$

$$\chi_1 = a_o + b_o\left(1 - \frac{U_v}{U_v^0}\right)$$

$$k_l a = k_l a_{\text{ref}}\left(\frac{N}{N_{ref}}\right)^{\alpha}$$

$$DP = \left(\frac{([E_g] + [E_a] + [E_v] + [E_{DEG}] + 2[Z])_{\text{feed}}}{[E_g] + [E_a] + [E_v] + [E_{DEG}]}\right)$$

Values of parameters/properties for the reference case

$$(k_1 a)_{\text{ref}} = 2.6875$$
$$\alpha = 2.6647$$
$$a_o = 1.0378$$
$$b_o = 2.1838$$
$$\rho_{EG} = 1{,}108 \text{ kg/m}^3$$
$$\rho_W = 1{,}000 \text{ kg/m}^3$$
$$\rho_{DEG} = 1{,}118 \text{ kg/m}^3$$

product property specifications. Such an intuitive ''feel'' of the system behavior is necessary to be able to ''guide'' *any* optimization code toward the optimal point or points, because of the narrow ''windows'' associated with the optimal solutions.

The two important objective functions for this system are the minimization of the acid and the vinyl end group concentrations, $[E_a]$ and $[E_v]$, respectively, in the product of the finisher. The acid end group makes the polymer susceptible to hydrolysis (Besnoin and Choi, 1989) during the downstream operations and leads to breakage of the filaments during spinning, where the humidity is very high. The vinyl end groups have been shown to be responsible for the coloration of PET (Besnoin and Choi, 1989; James and Packer, 1995), because of reactions not well understood right now, and not included in Table 1. Hence, the minimization of these two end groups improves the quality of the polymer product. The reduction of $[E_a]$ simultaneously increases the rate of polymerization of the acid end group catalyzed polycondensation reaction and helps maximize the throughput (this catalytic effect is not *directly* incorporated in the model, however). The important end-point constraint is to produce polymer with a desired value of the degree of polymerization (DP). Although the diethylene glycol (DEG) end groups affect the crystallinity and hence the melting point of the polymer unfavorably, they do improve the dyeability of the fiber. Therefore, it is preferred to have a certain allowable *range* for the concentration of DEG end groups in the fiber-grade polyesters. An inequality constraint is therefore imposed for the DEG end group concentration in the product, as per industrial requirements. In addition, a further inequality constraint on the maximum allowable limit for the acid end group concentration is imposed to ensure that it is not only minimized but also lies below an upper limit.

Table 3. Feed Conditions Used for Simulation

Feed concentrations (kmol/m³)	
$[E_g]_f = 4.0\times10^{-1}$	$[E_{DEG}]_f = 0.17$
$[E_a]_f = 2.57\times10^{-3}$	$[EG]_f = 6.5\times10^{-3}$
$[Z]_f = 11.2$	$[W]_f = 4.6\times10^{-4}$
$[E_v]_f = 1.17\times10^{-3}$	$[DEG]_f = 4.0\times10^{-4}$

Interestingly, it was found that the multiobjective optimization problem described earlier had a unique optimum solution, and that no Pareto set of several equally good optimal points was obtained. Also, it was found that the same values of the two objective functions were obtained for several sets of values of the operating conditions (values of the decision variables used) under optimal conditions, and so this optimization problem is associated with what we shall refer to as ''multiplicity.'' A suitable methodology was developed to study the problems associated with this multiplicity. Optimal solutions were generated for several values of the DP of the end product that had industrial significance, and it was found that there was considerable scatter in the results. This was due to the presence of multiplicity. A curve-fit procedure was developed to arrive at *near-optimal* solutions, which would be easier to implement in industry. We also found that the optimal solutions obtained for the preceding problem gave the lowest residence times of the reaction mass in the reactor, and so led simultaneously to a higher throughput from the continuous polymerization unit. A sensitivity analysis was performed to study the effect of the computational parameters. In addition, a few additional meaningful optimization problems were solved, and their results compared with those of the first problem.

Formulation

The mathematical model for the present study is based on the general step-growth polymerization kinetic scheme shown in Table 1. The reaction scheme consists of the main polycondensation reaction along with several side reactions. The side reactions lead to the formation of the extremely volatile acetaldehyde, A, the less volatile diethylene glycol, DEG, in the ''free'' form, and water, W. The other important side products produced are the acid and vinyl end groups, E_a and E_v, and E_{DEG}, the DEG end groups (''bound'' form). Besnoin and Choi (1989) have studied in detail the effect of these side products on the polymer quality. The various rate and equilibrium constants are also provided in Table 1. Some of these (k_{20}, k_{90}, K_1, K_5, and K_8) differ from those of Laubriet et al. (1991), and have been obtained by tuning the model for the reactor against industrial data (Bhaskar et al., 2000). The model equations (mass-balance equations for the liquid phase and the vapor–liquid equilibrium correlations) and values of some of the required parameters are given in Table 2. Details of the model development and the tuning of the model parameters for the industrial conditions are available elsewhere (Laubriet et al., 1991; Bhaskar et al., 2000). In general, the state-variable equations can be written in the form

$$dx/dz = f(x,u); \qquad x(z=0) = x_0, \tag{1}$$

where x is the vector of state variables, given by

$$x = \left[[E_g], [E_a], [Z], [E_v], [E_{\mathrm{DEG}}], [EG], [W], [DEG] \right]^T, \tag{2}$$

and u is the vector of control or decision variables. The variable, z, represents the (dimensionless) axial location.

Table 4. Computational Variables Used in this Study

Weightage factors	
$w_1 = w_3 = 10^4$;	$w_2 = 10^8$; $P_e = 10^4$
GA Parameters	
$N_{\mathrm{gen}} = 50$	$N_p = 50$
$p_c = 0.65$	$p_m = 0.004$
$\sigma = 3.0 \times 10^{-2}$	$\alpha_{sh} = 2.0$
$l_{\mathrm{chrom}} = 32$ bits	
Initial guess values used for y_j	
y_{EG} : 0.90	
y_w : 0.05	
y_{DEG} : 0.04	

The initial-value problem (IVP) given by the ordinary differential equations (ODEs) in Eq. 1 and given in Table 2 can be integrated using appropriate values of the feed conditions (given in Table 3). The IMSL subroutine, DIVPAG, is used to solve these equations. The subroutine uses Gear's algorithm (Gupta, 1995) with a tolerance (TOL) of 10^{-8}. An iterative solution is necessary to simulate the reactor for any set of conditions because the liquid and vapor phases have different kinds of flow (plug and well-mixed, respectively). Values for the *average* mol fractions, y_j, of three of the volatile species, EG, W, and DEG, in the vapor phase need to be assumed (see Table 4 for the first estimate values). The other volatile species acetaldehyde (A) is assumed to vaporize as soon as it is produced, and so, no assumption for y_A is required. Then, the ODEs are integrated from the dimensionless value of $z = 0$ (feed end) to $z = 1$ (product end). The well-mixed vapor phase values of y_j are then reevaluated and used as the estimate values for the next iteration. It is found that the method of successive substitutions (Picard iteration) (Gupta, 1995) converges for all the conditions studied. The iterations are continued till the sum of the squares of the y_j does not change by more than 1×10^{-12} between two successive iterations. The model provides values of DP as well as the concentrations of the hydroxyl end groups (E_g), acid end groups (E_a), diester groups (Z), vinyl end groups (E_v), DEG end groups (E_{DEG}), ethylene glycol (EG), water (W), and diethylene glycol (DEG), as functions of the axial position in the reactor after convergence is attained.

Five decision variables are used for optimization in this study. These are the reactor pressure (P), temperature (isothermal, T), catalyst concentration ($[Sb_2O_3]$), residence time of the polymeric reaction mass inside the reactor (θ), and the speed of the wiped-film agitator (N). All of these variables can easily be changed in any industrial, wiped-film reactor for PET manufacture, including the one being studied, and are therefore used to obtain the best optimal operating conditions.

The multiobjective function optimization problem described earlier and studied in this work is described mathematically by:

$$\text{Min } I(P, T, [Sb_2O_3], \theta^*, N^*) \equiv [I_1, I_2]^T = [[E_a]_{\mathrm{out}}, [E_v]_{\mathrm{out}}]^T \tag{3a}$$

subject to (s. t.)

$$DP_{\mathrm{out}} = DP_d \tag{3b}$$

$$[E_a]_{\text{out}} \le 1.038 \times 10^{-3} \text{ kmol/m}^3 \quad (3c)$$

$$0.1660 \le [E_{\text{DEG}}]_{\text{out}} \le 0.17 \text{ kmol/m}^3 \quad (3d)$$

$$dx/dz = f(x,u); \qquad x(z=0) = x_0 \quad (3e)$$

$$0.05 \le P \le 0.266 \text{ kPa } (0.4 \le P \le 2.0 \text{ mm Hg}) \quad (3f)$$

$$564 \le T \le 570 \text{ K} \quad (3g)$$

$$0.03 \le [Sb_2O_3] \le 0.045 \text{ wt. \%} \quad (3h)$$

$$0.90 \le \theta^* \le 1.06 \quad (3i)$$

$$0.93 \le N^* \le 1.05, \quad (3j)$$

where the subscripts *out* and *d* refer to the values at the outlet of the reactor and the desired values of the product property, respectively. The variables, θ^* and N^*, represent dimensionless values, $\theta/\theta_{\text{ref}}$ and N/N_{ref}, where θ_{ref} and N_{ref} are values being used currently in the industrial reactor being studied. These two values are confidential and are not being provided in this article for proprietary reasons. Meaningful bounds have been chosen on the five decision variables, u, based on industrial practice. These are given in Eqs. 3f–3j.

Several issues regarding the optimization problem formulated in this study need to be clarified and justified at this point. One is that we have used the catalyst concentration as a decision variable for the optimization of Stage 3 even though the catalyst is added (in the form of the glycolate) at the inlet of Stage 2. This has been done because the catalyst concentration used affects the operation of Stage 3 far more significantly than Stage 2, which is equilibrium-controlled (Ravindranath and Mashelkar, 1982) and is influenced primarily by the pressure and temperature used in that reactor. Since the catalyst is not consumed by the reactions, we could use the same catalyst concentration at the feed to Stage 2 as computed in our study of Stage 3 *alone*, and no correction is necessary. In fact, the catalyst concentration is usually measured in industry both at the inlet of the prepolymerizer and at the outlet of the finisher, and the difference is found to be below about 5%. Most of this difference is believed to be the catalyst carryover (vaporization) with the glycol that is removed at both stages (prepolymerizer and finisher). Also, use of catalyst concentration as a decision variable *while keeping the feed to the film reactor unchanged* is justified for the same reasons [product from Stage 2 depends on its pressure and temperature only, and is independent of the catalyst concentration, since the equilibrium constant is unchanged (Ravindranath and Mashelkar, 1986)]. The use of the residence time, θ^*, as a decision variable for the film reactor *while keeping the feed composition unchanged*, can be justified using similar arguments. We assume that a change in the residence time of the film reactor could be achieved by changing the flow rate of the reaction mass in this reactor (as well as in the previous two stages; this is the ''connectivity'' problem), rather than by changing the holdup volume of the melt in this reactor (which would lead to changes in the value of $k_l a$, something that is not well understood quantitatively). Since the first- as well as the second-stage reactors have considerable flexibility in industry, and since both these stages are equilibrium-controlled, a change in the flow rate does not necessarily lead to any changes in the composition of the feed to the film reactor. The choice of the five decision variables used in this study, and the use of constant feed conditions are thus justified and give us a great deal of flexibility for optimization, which can easily be implemented in industry.

The end-point constraint on DP (Eq. 3b) is incorporated in the form of a penalty function with a large value of the weightage factor, w_2 (10^8 in this study), as

$$\text{Min } I_1^* = w_1[E_a]_{\text{out}} + w_2\left(1 - \frac{DP_{\text{out}}}{DP_d}\right)^2 + P_e. \quad (4)$$

An additional large ''penalty'' value, P_e (10^4 in this study), is added to the objective function, I_1^*, if either of the two inequality constraints in Eqs. 3c and 3d (the maximum limit of the acid end group concentration at the outlet of the reactor, $[E_a]_{\text{out}}$, and the upper and lower bounds on the DEG end group concentration at the outlet of the reactor, $[E_{DEG}]_{\text{out}}$) are violated. If these constraints are satisfied, then the value of P_e in Eq. 4 is taken as zero. This ensures that bad chromosomes in the genetic algorithm used for optimization are not reproduced in the successive generations, even if several chromosomes violating these constraints exist in the initial population (that is, the chromosomes violating Eqs. 3c and 3d die out rapidly). Also, a very large value of P_e is added *if* the concentrations of three of the vaporizing species—EG, W, and DEG—in the vapor phase are higher than their respective vapor–liquid interfacial equilibrium concentrations—EG*, W*, and DEG*—at any axial location, in order to ensure the vaporization (rather than condensation) of these species at all axial locations. Minimization of I_1^* leads to a decrease in the acid end group concentration while simultaneously giving reference to solutions satisfying the several requirements just discussed. The use of a penalty to ''kill'' chromosomes when important physical constraints are violated is one of several adaptations of the basic algorithm suggested in this study.

The second objective function, I_2, is also modified to incorporate the penalties for the several constraints as discussed for I_1, and is given by

$$\text{Min } I_2^* = w_3[E_v]_{\text{out}} + w_2\left(1 - \frac{DP_{\text{out}}}{DP_d}\right) + P_e. \quad (5)$$

Minimization of the second objective function leads to a minimum value of the vinyl end group concentration in the product, thus reducing the product degradation due to thermal effects and improving the color of the polymer. It can be noted that $w_2 \gg w_1, w_3$. Use of w_1 and w_3 as 10^4 leads to values of $w_1[E_a]$ and $w_3[E_v]$ of the order of unity.

In our earlier parametric sensitivity study of this reactor (Bhaskar et al., 1999), we found that the two objective functions used here conflicted. Use of these functions was thus expected to lead to Pareto optimal solutions.

Results and Discussion

The solution of the multiobjective optimization problem described in Eq. 3 is obtained using the nondominated sorting genetic algorithm (NSGA; see the Appendix for a sum-

mary), as adapted by our group (Mitra et al., 1998), using values of the computational parameters as given in Table 4. This is referred to as the reference run. A software package was developed in FORTRAN90. The computer code was tested for a few simple two-objective function problems, as well as on some other problems, such as the optimization of steam reformers (Rajesh et al., 2000), membrane separation modules (Chan et al., 2000), and cyclone separators (Ravi et al., 1999), to ensure the correctness of the program. Then it was run for the PET wiped-film reactor. One of the optimal chromosomes obtained from the code was used in our earlier simulation code (Bhaskar et al., 2000). The same output variables were obtained from this as from the optimization code, thus confirming that the software package is free of errors. The CPU time taken on an SGI Origin 2000 supercomputer for one optimization run was 0.521 s.

The adapted NSGA code for the multiobjective optimization was first run for a DP_d of 82.0, the value corresponding to the reference case for the industrial reactor *simulated* earlier. Such a study would help explore whether changes in the operating variables could improve the performance of the industrial reactor. Figures 1 and 2 show all the feasible solutions (that is, those satisfying the end-point constraints in Eqs. 3b–3d) at different values of the generation number, N_g. In the initial generations, the feasible points are quite scattered in the $[E_a]_{out} - [E_v]_{out}$ space, but as the chromosomes evolve over the generations, the feasible points move toward a unique point. There are over 45 almost indistinguishable points in Figure 2 ($N_g = 50$). Therefore, the solution of our multiobjective function optimization problem with end-point constraints turns out to be unique, and is given by

$$[E_a]_{out} = 1.0 \times 10^{-3} \text{ kmol/m}^3$$
$$[E_v]_{out} = 7.549 \times 10^{-4} \text{ kmol/m}^3$$
$$DP_{out} = 82.000. \quad (6)$$

Table 5 shows the values of the five decision variables that correspond to the optimal point (reference run), as well as the corresponding values of several other product characteristics.

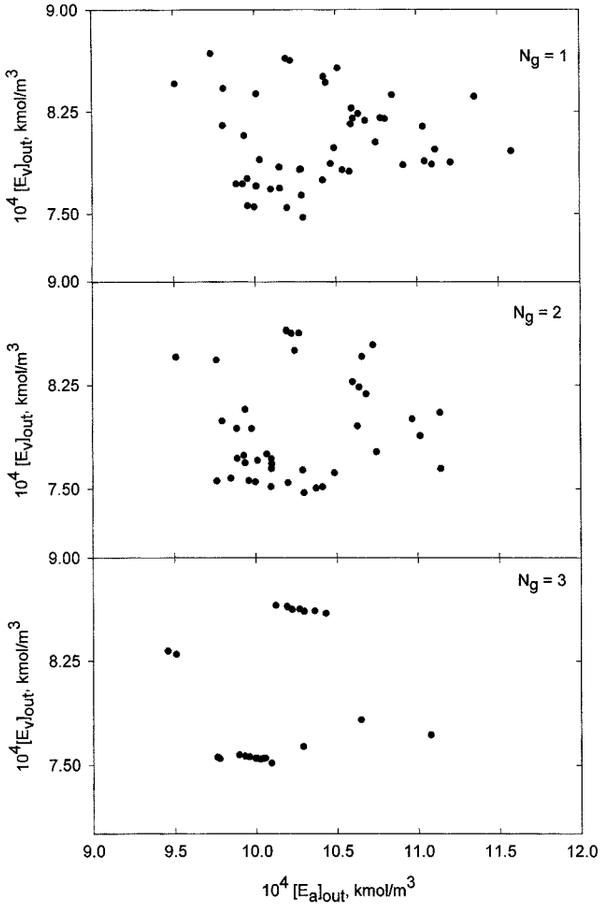

Figure 1. $[E_a]_{out}$ vs. $[E_v]_{out}$ for the feasible chromosomes for different values of the generation number, N_g.

The first three generations are shown.

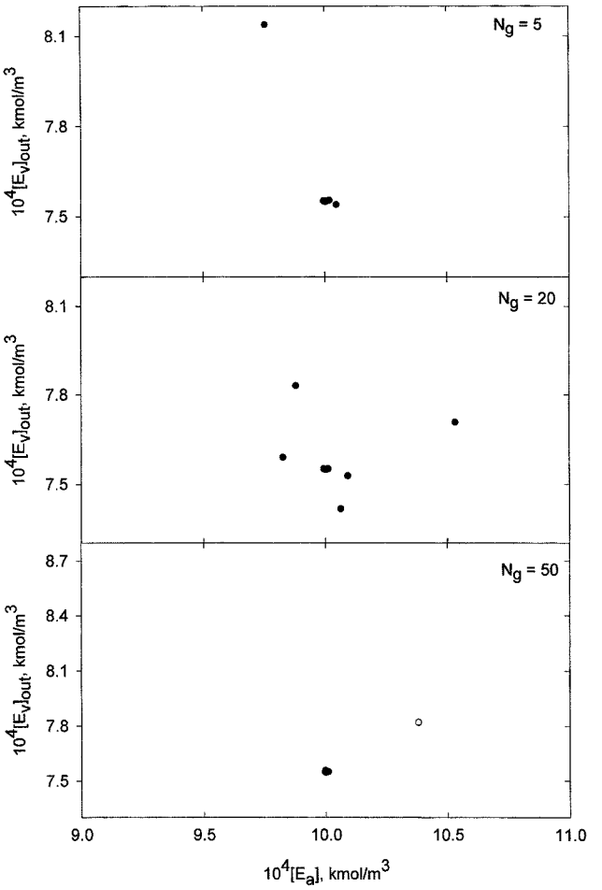

Figure 2. $[E_a]_{out}$ vs. $[E_v]_{out}$ for the feasible solutions for N_g = 5, 20 and 50.

The approach toward converged results is clearly indicated. The open circle for $N_g = 50$ represents the present operating condition of the industrial wiped-film reactor (Bhaskar et al., 1999).

Table 5. Optimal Operating Conditions and Product Properties for the Reference Run and Other Cases*

Operating Conditions	Optimal (Ref. Run)	Industrial	Near-Optimal	Effect of Feed	
				$[E_g]_f = 0.39$ kmol/m^3	$[E_g]_f = 0.41$ kmol/m^3
P, kPa (mm Hg)	0.185 (1.39)	0.266 (2.0)	0.133 (1.0)	0.137 (1.03)	0.115 (0.87)
T, K	564.02	566.0	565.03	565.35	564.25
10^2 [Sb_2O_3], wt. %	4.26	4.0	3.89	4.24	4.11
θ^*	0.9672	1.0	0.9907	0.9816	0.9322
N^*	1.0	1.0	1.004	0.9813	0.9776
Product Properties					
DP_{out}	82.00	82.00	82.11	82.00	82.00
$[E_g]_{out}$, kmol/m^3	0.1101	0.1091	0.1106	0.1054	0.1149
10^4 $[E_a]_{out}$, kmol/m^3	10.00	10.38	9.92	10.19	10.07
10^4 $[E_v]_{out}$, kmol/m^3	7.5	7.8	7.8	7.65	7.64
$[E_{DEG}]_{out}$, kmol/m^3	0.1682	0.1692	0.1674	0.1677	0.1676

*All the values given are for $DP_d = 82.0$ and $DP_f = 40.0$.

The uniqueness of the optimal solution is checked by performing an optimization using a single objective function. The objective functions, I_1^* and I_2^*, were taken one at a time, and optimal solutions were generated under the same conditions as given in Eqs. 3b–3j. The (unique) optimal solution obtained was found to be identical to that obtained from the NSGA. This means that minimizing either one of the side product concentrations, $[E_a]_{out}$ or $[E_v]_{out}$, simultaneously leads to a minimization of the other side product. This is quite interesting. In fact, similar unique solutions were obtained for other choices of DP_d, as discussed later. It should be emphasized that GA (as well as NSGA) is an extremely robust technique (Goldberg, 1989) and converges to the *global* optimal solution and also gives *all* the optimal solutions where several exist. It is possible that when a less robust technique is used to, say, minimize I_1, the corresponding value of I_2 may not be at the minimum value given by NSGA.

Figure 2 ($N_g = 50$) and Table 5 compare our optimal solution (indicated by filled circles) with the values corresponding to the current operation of the industrial wiped-film reactor (indicated by the open circle) (Bhaskar et al., 2000). It is observed that the optimal values of both the objective functions are, indeed, better than those obtained under the present operating conditions of the industrial reactor. Lower values for both the acid and vinyl end group concentrations are obtained using a lower value of the residence time ($\theta^* = 0.967$) and at a lower temperature. For the reactor under consideration, this decrease in θ^* corresponds to an increase of about 3–4% in the throughput without any major design modifications. The product is also of better quality. The lower temperature under optimal conditions would also lead to a reasonable amount of energy savings. As discussed earlier, the increase in the throughput can easily be achieved industrially by an increase in the rate of production of the prepolymer (in Stages 1 and 2), without affecting the feed concentrations of the film reactor. In fact, an operator in the plant has more flexibility to control the process variables in the earlier reactors than in the finishing reactor, since the operating conditions are far less severe in those reactors, and the product quality is not too sensitive to changes in the process variables.

Optimal solutions were then generated for several different choices of DP_d ranging from 80 to 84, values relevant to the fiber industry. These optimal solutions were generated using the same computational parameters (for reference values, see Table 4). In *all* of these cases, unique optimal solutions were obtained. The solutions are shown in Figures 3–5 (filled circles for different DP_d). Some amount of scatter is observed in these plots. The scatter in the optimal results was explored further. It has been suggested by Goldberg (1989) that even though GAs are quite efficient in reaching the global-optimum *region*, they are not guaranteed to reach the precise location of the global-optimum, particularly for complex problems, and may attain premature convergence. In fact, a similar scatter was observed earlier by Sareen and Gupta (1995) for an industrial nylon-6 reactor. The scatter was found to indicate the presence of compensating effects (interaction) of the several decision variables used in this study. We found that even in the case of the reference run (Figure 2, $N_g = 50$), use of different values of S_r, the seed for generating the sequence of random numbers, led to the same values of the two objective functions, but with *several* different sets of values of the five decision variables. We refer to this phenomenon as the problem of multiplicity. There are two methods of reducing this effect. One is to reduce the number of decision variables. This is not very desirable for industrial operations, since it eliminates the flexibility offered by the use of several decision variables where they are, indeed, available for control. Hence, it was decided to continue with the set of five decision variables and try some kind of ''smoothing'' of the results and obtain near-optimal solutions. Fortunately, it was found that the results were not *too* sensitive to small variations in the operating conditions. A linear curve fit of the plots (Figures 3–5) of the five decision variables, P, T, [Sb_2O_3], θ^*, and N^*, as a function of DP_d was performed. The curve-fit equations are given in Table 6. The properties, $[E_a]_{out}$, $[E_v]_{out}$, DP_{out}, $[E_g]_{out}$, and $[E_{DEG}]_{out}$, were then predicted using these curve-fit operating conditions in the simulation code (Bhaskar et al., 2000). The predicted results are also shown in Figures 3–5 (unfilled circles), *plotted as functions of* DP_{out} (rather than DP_d, since these two need not be the same for the curve-fitted case). Here we call

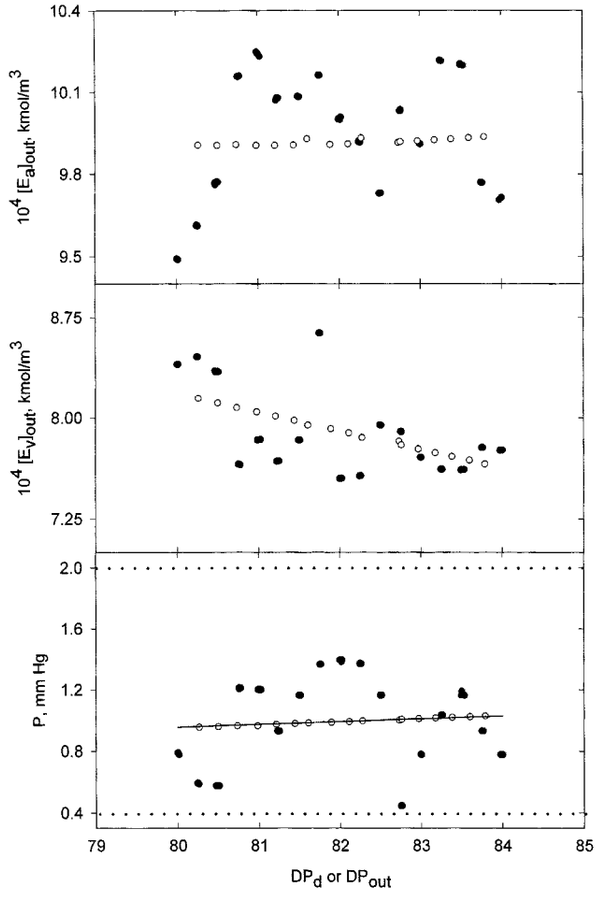

Figure 3. Optimum values of $[E_a]_{out}$, $[E_v]_{out}$, and P vs. DP_d (filled circles) as obtained using NSGA.

The open circles represent the *near-optimal* values of these variables as a function of DP_{out}, as predicted by the model simulation. The straight line in the last diagram represents the linear regression of P vs. DP_d (filled circles). The dotted lines represent the upper and lower bounds for the decision variable used.

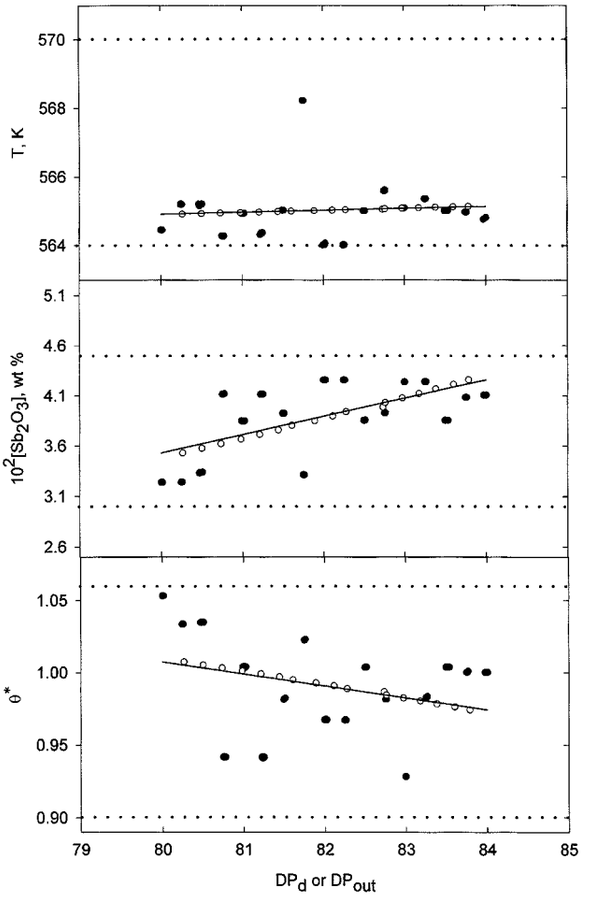

Figure 4. Optimum values of T, $[Sb_2O_3]$ and θ^* vs DP_d (filled circles) as obtained using NSGA.

The open circles represent the *near-optimal* values of these variables vs. DP_{out}, as predicted by the model simulation. The straight lines in the diagrams represent linear regressions of the decision variables, T, $[Sb_2O_3]$, and θ^*, vs. DP_d (filled circles). The dotted lines represent the upper and lower bounds for the decision variable used.

the solutions obtained using the curve-fit procedure *near-optimal* solutions. These near-optimal solutions are characterized by operating (decision) variables, which are less cumbersome to implement, and also lead to better values of $[E_a]_{out}$, $[E_v]_{out}$, and $[E_{DEG}]_{out}$. We recommend using these near-optimal charts because of their convenience. Smoothing the optimal solutions while keeping all the decision variables practically available to us, is an important adaptation offered in this study. It also could be used for other complex problems where the GA (or other algorithms) has premature convergence.

The optimum values of pressure and temperature predicted for the near-optimal solutions are about 0.133 kPa (1 mmHg) and 565 K. Figures 3–5 suggest that one can increase DP_{out} (without affecting the product quality) primarily by varying the catalyst concentration and the speed of the agitator. These actions are quite commonly practiced in industry.

We explored several other optimization problems besides that given in Eq. 3. Since minimizing $[E_a]_{out}$ simultaneously minimizes $[E_v]_{out}$, we tried to minimize θ^* and $[E_v]_{out}$ instead to see if Pareto solutions are obtained. The exact problem studied is given by

$$\text{Min } I(P, T, [Sb_2O_3]\theta^*, N^*) \equiv [I_1, I_2]^T = [\theta^*, [E_v]_{out}]^T$$
$$\text{s.t.}$$
$$\text{Eqs. 3b–3j.} \qquad (7)$$

Minimizing θ^* leads to an increase in the throughput while minimizing $[E_v]_{out}$ (and thus $[E_a]_{out}$) improves the product quality. Once again, unique optimal solutions were obtained for different values of DP_d. In fact, the optimal solutions were exactly the same as those obtained for the problem described by Eq. 3. It is interesting to observe that minimizing $[E_a]_{out}$ and/or $[E_v]_{out}$ simultaneously minimizes θ^*, which leads to a higher throughput. This is not really surprising, since minimization of $[E_a]$ throughout the reactor (which accompanies

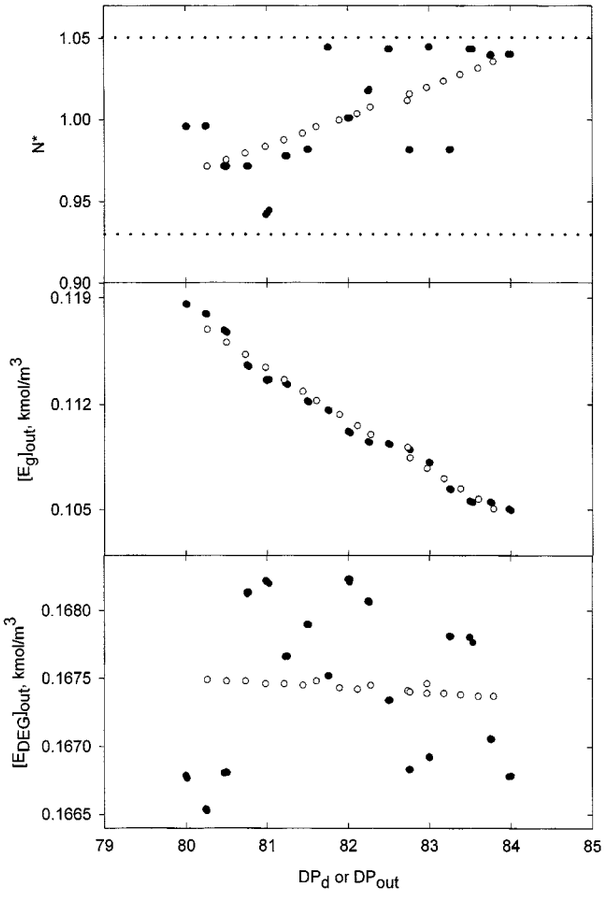

Figure 5. Optimum values of N^*, $[E_g]_{out}$, and $[E_{DEG}]_{out}$ vs. DP_d (filled circles) as obtained using NSGA.

The open circles represent the *near-optimal* values of these variables vs. DP_{out} as predicted by the model simulation. The straight line in the first diagram represent the linear regression of N^* vs. DP_d (filled circles). The dotted lines represent the upper and lower bounds for the decision variable used.

minimization of $[E_a]_{out}$) simultaneously leads to an increase in the rate of polymerization (Besnoin and Choi, 1989). In fact, reaction 9 in Table 1 suggests that minimization of $[E_a]$ and $[E_v]$ will lead to a suppression of this reaction, and thus to higher values of $[Z]$, which in turn leads to faster attainment of DP_d. The simultaneous minimization of three objective functions $[E_a]_{out}$, $[E_v]_{out}$, and θ^* using NSGA would thus be expected to lead to a unique optimal point, also.

We next tried to fix some of the decision variables at their current operating conditions of the industrial reactor, and solved the 2-objective function optimization problem given below:

$$\text{Min } I(T, \theta^*) \equiv [I_1, I_2]^T = [[E_a]_{out}, [E_v]_{out}]^T \quad (8a)$$

s.t.

$$DP_{out} = DP_d = 82.0 \quad (8b)$$

Eqs. 3c–3e, 3g, 3i (8c)

$$P = 0.266 \text{ kPa (2.0 mm Hg)} \quad (8d)$$

$$[Sb_2O_3] = 0.04 \text{ wt. \%} \quad (8e)$$

$$N^* = 1.0. \quad (8f)$$

Once again, a unique optimal solution is obtained. Interestingly, the optimal operating temperature and the residence time were found to be the same as the values currently used in both the industrial reactor, and in our previous study (Bhaskar et al., 2000). This indicates that the present industrial reactor is, indeed, operating at its optimal condition when the three decision variables, P, $[Sb_2O_3]$, and N^*, are *constrained* to lie at their *current* (operating) values. However, improvements are possible if these constraints are removed.

We also explored the effect on the optimal solutions of varying the feed concentrations (while keeping DP_f constant, somewhat arbitrarily, at 40.0). Since the feed to the finishing reactor could be varied by changing the process conditions (pressure, temperature) in the prepolymerizer, such a preliminary study gives us some insights about whether it would be useful to carry out a more elaborate system-optimization, using models for all three reactors used in the process. Some information on this was obtained from the work of Saint Martin and Choi (1991), who studied the effect of the feed conditions on the DP of the product and the EG removal rate. Since DP_f was fixed at 40, we varied $[E_g]_f$ (which, in turn, alters the value of $[Z]_f$). The multiobjective optimization problem (described by Eqs. 3a–3j) is solved for two different concentrations of $[E_g]_f$ (0.39 and 0.41 kmol/m^3). The effect of other feed concentrations was not found to be too significant and the polycondensation reaction is controlled primarily by $[E_g]_f$ and $[Z]_f$. The results are tabulated in Table 5, which suggests (see results for $[E_g]_f = 0.41$ kmol/m^3) that a more detailed system optimization could possibly provide higher throughputs (lower θ^*), while giving values of $[E_a]_{out}$ and $[E_v]_{out}$ that are only slightly worse than those obtained for the present case.

Since NSGA involves several computational parameters, it is very important to analyze how the final results are affected by variations in these computational parameters. The computational parameters involved are the number of generations, N_g, the number of chromosomes, N_p, chromosome length, l_{chrom}, the seed, S_r, used for the random number generator, the two parameters involved in controlling the niche count of each of the chromosomes (α_{sh}, the exponent controlling the sharing effect, and σ, the maximum normalized distance in u-space between any two points), crossover probability, p_c,

Table 6. Curve-Fit Equations for Decision Variables*

	$u_i = a_i + b_i(DP_d)$	
u_i	a_i	b_i
P, kPa (mm Hg)	-69.99×10^{-3} (-0.5251)	2.466×10^{-3} (0.0185)
T, K	560.45	0.0558
$10^2[Sb_2O_3]$, wt. %	-11.071	0.1825
θ^*	1.6678	-8.257×10^{-3}
N^*	-0.3065	0.0160

* Units of a_i and b_i are consistent with those of u_i.

mutation probability, p_m, and the weightage factors, w_1, w_2, and w_3, used in the penalty functions. The effect of N_g was presented in Figures 1 and 2. It is clear that the maximum number of generations (which is used as the termination criterion) should be set high enough to ensure convergence, while not too high to avoid wastage of computational time.

The population size, N_p, has to be large enough to allow diversity in the population. Too low a value of N_p leads to erroneous results. The final results were found to be unaffected if N_p was increased from 50 to 200. Therefore, $N_p = 50$ was used in this study. The length of the chromsome, l_{chrom}, affects the accuracy of the solution. The length of the chromosome used in this study was 160 bits (5 decision variables $\times 32$ bits each). Increase in l_{chrom} did not lead to changes in the results. No significant change in the final values of the objective functions was obtained if S_r was varied, but the effect of multiplicity was observed, as described earlier. It was also observed that the final results were quite insensitive to α_{sh}, the exponent that controls the sharing effect (Srinivas and Deb, 1995). The maximum niche-count distance, σ, would have played a more important role if the solutions for this multiobjective optimization problem had been a Pareto set, since this parameter affects the spread of solutions on the Pareto set. Since a unique optimal solution was obtained for this problem, σ has a negligible effect on the final results.

The two most important parameters that influence the course of NSGA are the crossover, p_c, and mutation, p_m, probabilities. Figure 6 describes the effect of the crossover probability in the range of 0.6 to 0.7. The rate at which the final solution is attained was different for different values of the crossover probability, but the final results were not affected by its choice, at least in the range studied. A crossover probability of 0.65 (reference value) was used in this study. The mutation probability was varied from 0.0 to 0.005, and it was found to only marginally affect the final solution. As expected, better results were obtained if a nonzero value of the mutation probability was used. The optimum value of $[E_a]_{\text{out}}$ and $[E_v]_{\text{out}}$ are 1.024×10^{-3} kmol/m^3 and 7.59×10^{-4} kmol/m^3, respectively, when $p_m = 0$, compared to 1.0×10^{-3} kmol/m^3 and 7.549×10^{-4} kmol/m^3 for values of p_m of 0.004 and 0.005. A (reference) value of p_m of 0.004 was used in this study for the other cases.

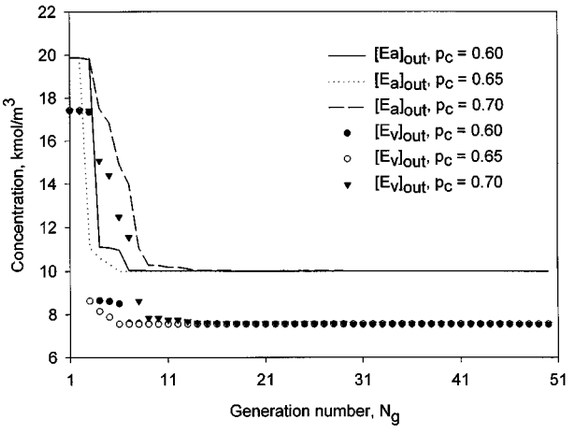

Figure 6. Effect of crossover probability on the convergence of the solution.

The plot represents the concentrations of acid and vinyl end groups in the product (minimum among all the chromosomes in each generation) vs. N_g.

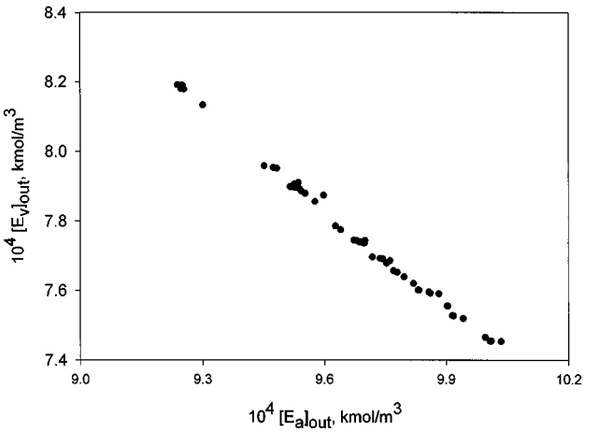

Figure 7. Plot of $[E_a]_{\text{out}}$ vs. $[E_v]_{\text{out}}$ showing the effect of the weightage factor, w_2, ($=10^3$) on the optimal solution.

The effect of the three weightage factors, w_1, w_2, and w_3, was also studied. It was observed that w_1 and w_3 do not affect the final results much. In fact, w_1 and w_3 are used only to obtain the values of the order-of-unity objective function. In contrast, w_2 affects the nature of the solution tremendously. Lower values of w_2 ($<10^8$), do not give rise to a unique solution, since they permit (and give) deviations of DP_{out} from DP_d (of ± 0.15 for $w_2 = 10^3$). Such deviations are usually not desired in the industrial scenario, at least under steady-state conditions. Figure 7 shows the variation of $[E_a]_{\text{out}}$ with $[E_v]_{\text{out}}$ for $w_2 = 10^3$. A considerable amount of scatter is observed in plots of the decision variables vs. $[E_a]_{\text{out}}$. Figure 7 should not be mistaken for a Pareto set, since the requirement of $\text{DP}_{\text{out}} = \text{DP}_d$ is not satisfied precisely (the error is ± 0.15). Lower values of the penalty, P_e, are not preferred because we do not want the "bad" chromosomes to get reproduced in the successive generations. If P_e was decreased from 10^4 to 10^3, the constraints in Eq. 3 would be violated by most of the chromosomes in the population.

The present study emphasizes the importance of obtaining better correlations for the optomechanical properties (for example, color, melt index, fiber strength) in terms of the concentrations of the different chemical species present in the polymer product. A better understanding of these correlations would lead to improved optimal designs and operation. This was emphasized by Bokis et al. (1999) when they addressed the problems involving the modeling of polymerization processes for commercial simulators.

Conclusions

Minimization of the degradation side products, $[E_a]_{\text{out}}$ and $[E_v]_{\text{out}}$, was carried out using an adapted NSGA technique. P, T, $[Sb_2O_3]$, θ^*, and N^* were used as the decision variables. An end-point constraint was imposed on DP_{out}, while the concentration, $[E_a]_{\text{out}}$, was constrained to lie below a maximum value. In addition, an allowable range was pre-

scribed for $[E_{DEG}]_{out}$. A unique solution was obtained for this multiobjective optimization problem. No Pareto set of noninferior solutions was obtained. Unique optimal solutions were generated for a range of values of DP_d that are of importance in the polyester fiber industry. Optimal control variable charts were constructed for producing polymers with different values of DP_{out} that are less cumbersome to use, by using a smoothening procedure. It was found that minimizing $[E_a]_{out}$ and/or $[E_v]_{out}$ simultaneously leads to a minimization of the residence time, θ^*. The operation of an industrial reactor is discussed in reference to our optimal solutions.

Acknowledgment

One of the authors (S.K.G.) gratefully acknowledges the hospitality and kindnesses (and the excellent infrastructure) that he is enjoying as a Visiting Professor at the University of Wisconsin, Madison, where this article was revised.

Notation

a = specific interfacial area per unit volume of the melt, m^{-1}
A_1 = cross-sectional area of the melt in the reactor, m^2
a_0, b_0 = parameters in the equation describing χ_1
C_j = concentration of the volatile species, j, in the melt (= $[j]$), kmol/m^3
C_j^* = equilibrium concentration of the volatile species, j, in the melt at the interface, kmol/m^3
C_{poly} = total concentration of the polymeric species in the melt and at the interface, kmol/m^3
I = vector of objective functions
k_1 to k_9 = forward reaction rate constants for Eqs. 1–9 in Table 1
k'_1, k'_5, k'_7, k'_8 = reverse reaction rate constants for Eqs. 1, 5, 7 and 8 in Table 1
k_{20}, k_{90} = frequency factors of Eqs. 2 and 9 (Table 1), respectively
k_l = overall liquid phase mass-transfer coefficient, m/min
L = length of the reactor, m
M_j = molecular weight of the volatile species, j
m_j = ratio of liquid-phase molar volumes of the polymer and pure species, j
P_j^0 = vapor pressure of species j, mmHg
Q = volumetric flow rate of liquid in the reactor, m^3/min
R = universal gas constant = 8.314 J/(mol·K)
R_1 to R_9 = reaction rate terms
U_v = volume fraction of volatile material in the melt
U_v^0 = volume fraction of volatile material in the melt at $z = 0$
V_p = molar volume of pure liquid polymer, kmol/m^3
x_j^* = melt-phase mol fraction of the volatile species, j, at the interface (at equilibrium)
α = exponent describing the effect of agitator speed on $k_l a$
γ_j = activity coefficient of the volatile species, j
ρ_j = density of the pure liquid species, j, kg/m^3
χ_1 = Flory-Huggins' polymer–solvent interaction parameter

Symbols

$[\cdot]$ = concentration in the melt, kmol/m^3 (unless otherwise specified)

Subscripts

ref = reference conditions as in Bhaskar et al. (1999)
f = feed value

Literature Cited

Besnoin, J. M., and K. Y. Choi, "Identification and Characterization of Reaction Byproducts in the Polymerization of Polyethylene Terephthalate," *J. Macromol. Sci. Rev. Macromol. Chem. Phys.*, **C29**, 55 (1989).

Bhaskar, V., S. K. Gupta, and A. K. Ray, "Modeling of an Industrial Wiped Film Poly (Ethylene Terephthalate) Reactor," *Polym. React. Eng.*, in press (2000).

Bokis, C. P., H. Orbey, and C. C. Chen, "Properly Model Polymer Processes," *Chem. Eng. Prog.*, **95**, 39 (1999).

Butala, D., K. Y. Choi, and M. K. H. Fan, "Multiobjective Dynamic Optimization of a Semibatch Free-Radical Copolymerization Process with Interactive CAD Tools," *Comput. Chem. Eng.*, **12**, 1115 (1988).

Chakravarthy, S. S. S., D. N. Saraf, and S. K. Gupta, "Use of Genetic Algorithms in the Optimization of Free Radical Polymerizations Exhibiting the Trommsdorff Effect," *J. Appl. Poly. Sci.*, **63**, 529 (1997).

Chan, C. Y., Aatmeeyata, S. K. Gupta, and A. K. Ray, "Multiobjective Optimization of Membrane Separation Modules," *J. Memb. Sci.*, in press (2000).

Chankong, V., and Y. Y. Haimes, *Multiobjective Decision Making —Theory and Methodology*, Elsevier, New York (1983).

Choi, K. Y., and D. N. Butala, "An Experimental-Study of Multiobjective Dynamic Optimization of a Semibatch Copolymerization Process," *Poly. Eng. Sci.*, **31**, 353 (1991).

Deb, K., *Optimization for Engineering Design: Algorithms and Examples*, Prentice Hall of India, New Delhi (1995).

Fan, L. T., C. S. Landis, and S. A. Patel, *Frontiers in Chemical Reaction Engineering*, L. K. Doraiswamy and R. A. Mashelkar, eds., Wiley Eastern, New Delhi, p. 609 (1984).

Farber, J. N., "Steady State Multiobjective Optimization of Continuous Copolymerization Reactors," *Poly. Eng. Sci.*, **26**, 499 (1986).

Farber, J. N., *Handbook of Polymer Science and Technology*, Vol. 1, N. P. Cheremisinoff, ed., Dekker, New York, p. 429 (1989).

Garg, S., and S. K. Gupta, "Multiobjective Optimization of a Free Radical Bulk Polymerization Reactor Using Genetic Algorithm," *Macromol. Theor. Simul.*, **8**, 46 (1999).

Garg, S., S. K. Gupta, and D. N. Saraf, "On-Line Optimization of Free Radical Bulk Polymerization Reactors in the Presence of Equipment Failure," *J. Appl. Poly. Sci.*, **71**, 2101 (1999).

Goicoechea, A., D. R. Hansen, and L. Duckstein, *Multiobjective Decision Analysis With Engineering and Business Applications*, Wiley, New York (1982).

Goldberg, D. E., *Genetic Algorithms in Search, Optimization and Machine Learning*, Addision-Wesley, Reading, MA (1989).

Gupta, R. R., and S. K. Gupta, "Multiobjective Optimization of an Industrial Nylon-6 Semibatch Reactor System Using Genetic Algorithm," *J. Appl. Poly. Sci.*, **73**, 729 (1999).

Gupta, S. K., *Numerical Methods for Engineers*, New Age International, New Delhi (1995).

Immanuel, C. D., and S. K. Gupta, "Optimization of the First Stage Continuous Reactor-Sequence in Polyester Manufacture from Purified Terephthalic Acid," *J. Poly. Eng.*, (1999).

James, D. E., and L. G. Packer, "Effect of Reaction Time on Poly(Ethylene Terephthalate) Properties," *Ind. Eng. Chem. Res.*, **34**, 4049 (1995).

Kumar, A., S. N. Sharma, and S. K. Gupta, "Optimization of Polycondensation Step of PET Formation with Continuous Removal of Condensation Products," *Poly. Eng. Sci.*, **24**, 1205 (1984a).

Kumar, A., S. A. Sharma, and S. K. Gupta, "Optimization of Polycondensation Stage of PET Reactor," *J. Appl. Poly. Sci.*, **29**, 1045 (1984b).

Kumar, A., V. K. Sukthankar, C. P. Vaz, and S. K. Gupta, "Optimization of the Transesterification of PET Reactor," *Poly. Eng. Sci.*, **24**, 185 (1984c).

Laubriet, C., B. LeCorre, and K. Y. Choi, "Two-Phase Model for Continuous Final Stage Melt Polycondensation of Poly(Ethylene Terephthalate): 1. Steady-State Analysis," *Ind. Eng. Chem. Res.*, **30**, 2 (1991).

Mitra, K., K. Deh, and S. K. Gupta, "Multiobjective Dynamic Optimization of an Industrial Nylon 6 Semibatch Reactor Using Genetic Algorithm," *J. Appl. Poly. Sci.*, **69**, 69 (1998).

Rajesh, J. K., S. K. Gupta, G. P. Rangaiah, and A. K. Ray, "Multiobjective Optimization of Steam Reformer Performance Using Genetic Algorithm," *Ind. Eng. Chem. Res.*, **39**(3), 706 (2000).

Ravi, G., S. K. Gupta, and M. B. Ray, "Multiobjective Optimization of Cyclone Separators," *Ind. Eng. Chem. Res.* (1999).

Ravindranath, K., and R. A. Mashelkar, "Modeling of Polyethylene

Terephthalate Reactors: 5. A Continuous Prepolymerization Process," *Poly. Eng. Sci.*, **22**, 619 (1982).
Ravindranath, K., and R. A. Mashelkar, "Finishing Stages of PET Synthesis: A Comprehensive Model," *AIChE J.*, **30**, 415 (1984).
Ravindranath, K., and R. A. Mashelkar, "Polyethylene Terephthalate-I. Chemistry, Thermodynamics and Transport Properties," *Chem. Eng. Sci.*, **41**, 2197 (1986).
Saint Martin, H. S., and K. Y. Choi, "Two-Phase Model for Continuous Final Stage Melt Polycondensation of Poly (ethylene terephthalate). 2. Analysis of Dynamic Behavior," *Ind. Eng. Chem. Res.*, **30**, 1712 (1991).
Sareen, R., and S. K. Gupta, "Multiobjective Optimization of an Industrial Semibatch Nylon 6 Reactor," *J. Appl. Poly. Sci.*, **58**, 2357 (1995).
Srinivas, N., and K. Deb, "Multiobjective Function Optimization Using Nondominated Sorting Genetic Algorithms," *Evol. Comput.*, **2**, 3 (1995).
Tieu, D., W. R. Cluett, and A. Penlidis, "Optimization of Polymerization Reactor Operation: Review and Case Studies with the End-Point Collocation Method," *Poly. React. Eng.*, **2**, 275 (1994).
Tsoukas, A., M. V. Tirrell, and G. Stephanopoulos, "Multiobjective Dynamic Optimization of Semibatch Copolymerization Reactors," *Chem. Eng. Sci.*, **37**, 1785 (1982).
Wajge, R. M., and S. K. Gupta, "Multiobjective Dynamic Optimization of a Nonvaporizing Nylon-6 Batch Reactor," *Poly. Eng. Sci.*, **34**, 1161 (1994).

Appendix 1: Short Note on NSGA

Deb and Srinivas (1995) developed the Nondominated Sorting Genetic Algorithm (NSGA) to solve multiobjective optimization problems. This algorithm generates a set of solutions that are nondominating over each other. Two solutions are said to be nondominating if on moving from one point to another we find an improvement in one of the objective functions but a deterioration in one (or more) of the other objective function(s). The final set of nondominating solutions is referred to as a Pareto-optimal set. This algorithm differs from the simple GA (Goldberg, 1989; Deb, 1995) in the way the selection operator works. In the NSGA, the randomly generated solutions are sorted into fronts—an imaginary enclosure within which all the chromosomes present are mutually nondominating. Such fronts are assigned progressively lower common (dummy) values of the fitness function. Each chromosome in any front is then assigned an individual value of the fitness function. This is obtained by dividing the dummy fitness value for the front by the niche count of the individual chromosome, a parameter proportional to the number of chromosomes in its neighborhood (in the decision variable space) within the same front. This action helps to spread out the chromosomes while maintaining the diversity of the gene pool. All other operations performed are similar to those in the traditional GA. The relevant GA parameters used in this study are presented in Table 4. Figure A1 (Mitra et al., 1998; and Garg and Gupta, 1999) describes NSGA.

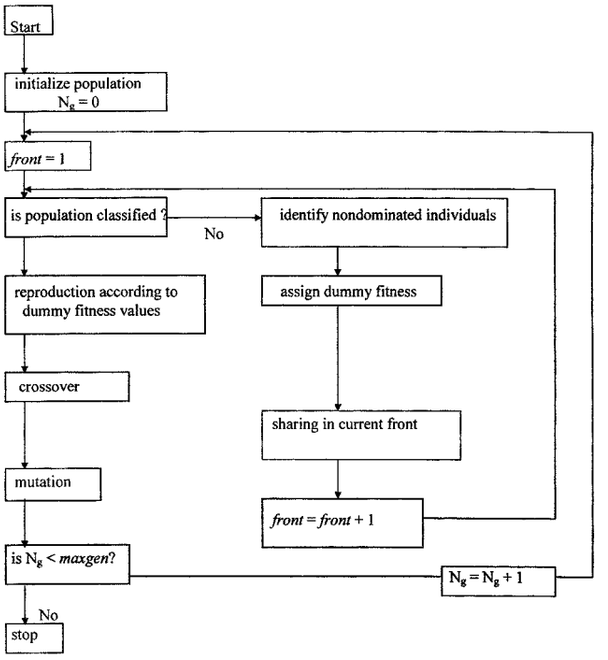

Figure A1. Adapted NSGA.

Manuscript received July 21, 1999 and revision received Nov. 29, 1999.